

Surface Emissivity Effect on the Performance of Composite Metal Foam against Torch Fire Environment

Nigel Thomas Amofo-Yeboah¹ and Afsaneh Rabiei^{1,a*}

¹Mechanical and Aerospace Engineering, 1840 Entrepreneur Drive, Raleigh NC 27606, United States of America

^arabiei@ncsu.edu

Keywords: Surface Emissivity, Composites, Torch Fire, Metal Foams

Abstract. According to the US Department of Transportation (DOT), there are millions of liters of hazardous materials (HAZMATs) transported each year via railroad. This has translated to stringent safety measures taken to alleviate the effects of accidents involving tank cars carrying these HAZMATs. One of such measures is in the creation of the thermal protection system of tank cars in which the tank car must have sufficient thermal resistance when subjected to a simulated pool fire for 100 mins and a torch fire for 30 mins without its back plate temperature exceeding 427 °C at any point of time. This requires a suitable material as a thermal blanket and insulation in tank car lining. Steel-steel composite metal foam (S-S CMF) is a novel metal foam with unique properties of high strength to density ratio, lightweight, and high energy absorption. It consists of metallic hollow spheres that are closely packed within a metal matrix. The large percentage of air within the hollow spheres provide both lightweight and insulating effects for CMF. S-S CMF is being investigated using the standard torch fire test requirement to determine its suitability as a material for tank car thermal protection. This is accomplished by developing a numerical model using the Fire dynamics simulator (FDS) as a form of validation for experimental work done. To properly evaluate this, there are various thermal properties of S-S CMF that need to be established for predicting CMF's thermal response. Surface emissivity has been a challenging property to evaluate and hence this study focuses on developing an experimental and numerical procedure in evaluating this property for composite materials such as CMF. Preliminary data shows an acceptable prediction of emissivity, which will be applied to the FDS model for the torch fire test.

1. Introduction

Safety in the transportation industry has been a major interest for the US Department of Transportation (DOT), specifically in transportation of hazardous materials (HAZMATs). Currently the DOT have developed the DOT117 tank car with the DOT 117R standard specifications for thermal protection [1]. This specification requires the tank car to have sufficient thermal resistance when subject to a simulated pool fire for 100 mins and a torch fire for 30 mins [2]. Steel-Steel composite metal foam (S-S CMF) is a composite material that exhibits superior thermal properties as proven in some research studies [3], [4]. This material is being investigated for its potential use in these tank cars, as a partial replacement for the current configuration where ceramic wool is sandwiched by thick and heavy layers of carbon steel. So far, S-S CMF has successfully passed a pool fire and a small-scale torch fire test by a large margin [3][5]. However, since the desired goal is to have a full-scale torch fire test, it became necessary to develop a numerical method to expand upon data obtained from the small-scale experimental work. This is achieved using a fire-driven flow computational software known as the Fire Dynamics Simulator (FDS). This attempt requires modeling the S-S CMF by having known physical and thermal properties such as density, thermal conductivity, emissivity, and specific heat capacity. Due to the diverse parameters affecting the surface roughness of complex surfaces of composite metal foam, its surface emissivity measurements tend to pose a challenge when being experimentally evaluated

or analytically extrapolated. This study seeks to establish an experimental method for deriving surface emissivity, that is applicable to composite materials.

2. Materials and processing

The S-S CMF samples were manufactured using stainless steel hollow spheres embedded in a 316L stainless steel matrix. The lost core technique was used to manufacture hollow steel spheres with an average outer diameter of 2 mm with wall thickness of about 100 μm [6]. The spheres were manufactured in Dresden, Germany, by Hollomet GmbH. The hollow steel spheres were shaken into a random-loose packing arrangement within a steel mold surrounded by 316L stainless steel powder from North American Höganäs, with an average particle size of 44 μm . The mold was then heated in a vacuum hot press and allowed to cool under a high vacuum to room temperature. The elemental composition of these samples is shown in Table 1.

After this, samples were then extracted, cleaned, and ground to create a flat surface and uniform thickness. Samples of cylindrical shape with dimensions of diameter 25.59 mm and height 25.26 mm were produced for this surface emissivity measurement. The samples were further ground on 180, 600 and 1200 grit sand paper.

Table 1. Chemical composition of S-S CMF components by weight percent

Material	Chemical composition (weight percent)						
	Fe	C	Mn	Si	Cr	Ni	Mo
2mm diameter Steel Spheres	Balance	0.68	0.13	0.82	16.11	11.53	2.34
316L Steel Matrix	Balance	0.03	2.00	1.00	16.00-18.00	10.00-14.00	2.00-3.00

3. Experimental procedure

3.1 Emissivity measurements

This section describes the test set up as well as the experimental procedure in determining emissivity of the S-S CMF samples. As a composite material, the S-S CMF is made up of spheres and matrix in between, and hence in determining the global emissivity, the emissivity's of the spheres and matrix were found separately and then put together using the rule of mixtures.

3.1.1 Test set up and measurement procedure for CMF matrix emissivity

The set up was developed in accordance with ASTM standard E1933—14 Standard Practice for Measuring and Compensating for Emissivity using Infrared Imaging radiometers [7]. For these tests the contact thermometer method was used. For emissivity measurements a FLIR E40 infrared radiometer camera was used. A Thermo Scientific Thermolyne HPA2235MQ analog hot plate was used as a primary heat source, with the CMF sample placed in a ceramic insulation block surrounding the perimeters of the cylinder, leaving the top surface exposed towards the IR camera and the bottom surface in direct contact with the hotplate. Two type R thermocouples were placed on the matrix surface of the sample for temperature measurements and were connected to a national instruments cDAQ 9171 data acquisition unit. The national instruments cDAQ was connected to a computer and LabVIEW software for the analysis of temperature data. An enclosure with a black interior was built to house the hotplate and sample, to prevent external reflections that could affect accuracy of the data acquisition. Figure 1 shows the test set up for the emissivity measurements. The set up was calibrated, by measuring emissivity of a flat stainless-steel sample from room temperature to 200 °C, resulting in data consistent with known emissivity values for stainless-steel.

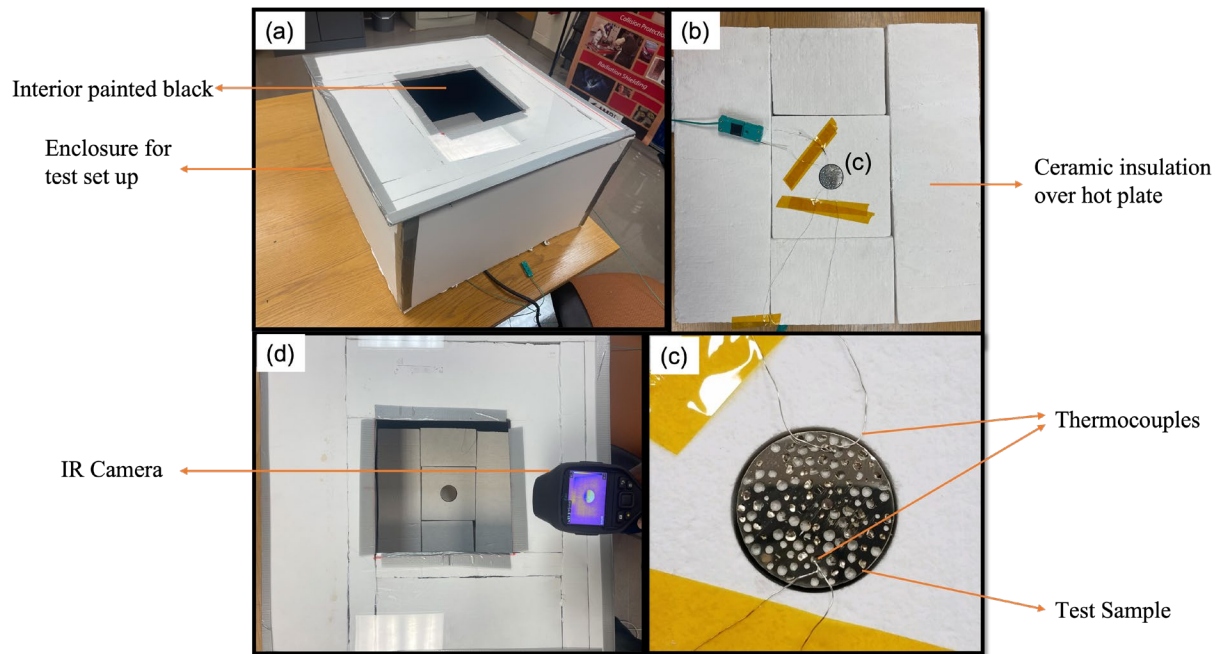


Figure 1. (a) Overview of test set up (b) Image showing ceramic insulation on hot plate (c) CMF sample with thermocouples (d) IR camera reading emissivity data

To record emissivity data for the CMF matrix, the sample was heated from room temperature to 200 °C in increments of 50 °C. At each temperature increment, the FLIR IR camera was positioned to measure the temperature of the CMF matrix surface, and emissivity value on the IR camera adjusted till the camera temperature readings matched that off the temperature from the thermocouples. This adjusted emissivity value then becomes the emissivity of the CMF matrix at that temperature. This procedure was repeated for the various grit sizes of 180, 600 and 1200 to investigate the effect of surface roughness on emissivity. Results obtained from these measurements are discussed in the results section.

3.1.2 Measurement procedure for sphere emissivity

The second part of the procedure involves establishing a method for determining the emissivity of the spheres. Since the spheres are randomly packed in the matrix, and are cut at various sections, spheres are seen on the surface with varying depths, however this method does not take into consideration those different depths of spheres that are exposed on the top surface. However, an indirect method is adapted to measure the sphere emissivity's. This involves measuring the surface roughness of the spheres and then producing this roughness on a regular 316L stainless steel sample using the sand blasting method. These roughness measurements were done using a Keyence VKx1100 optical profilometer. This device scans the sample by shooting a laser to detect the height (z) information across the x and y planes of the sample surface and gives a roughness (Ra) value for the profile. This was done multiple times across the x and y plane to give an average Ra value. After measurements were done, the average Ra valued obtained for the sphere surface was 5.4 μm , whilst that of the sandblasted sample was 6.8 μm , translating to close enough values for emissivity measurements. Once matching the surface roughness of the interior surfaces of spheres and the sandblasted sample were successful, emissivity measurements were conducted on the sand blasted sample at temperatures between room temperature and 250 °C. Table 2 shows raw data obtained for emissivity obtained after measurement.

Table 2. Emissivity measurements obtained for Sand Blasted sample.

Emissivity measurement for sand blasted sample	
Temperature (°C)	Emissivity
50	0.8
100	0.8
150	0.75
200	0.63
250	0.58

3.1.3 Effects of sphere curvature on emissivity

Emissivity is affected by several factors, one of which is the angle of measurement which is depicted in figure 2. Since sphere emissivity's are being measured indirectly, it was needful to come up with a numerical formulation to take into consideration the effects of the spheres interior surface curvatures on the global sphere emissivity. This was achieved by generating an equation based on a compilation of available literature data on the effect of measurement angle on 316L stainless steel [8][9][10]. These literature sources derived similar equations, and hence were numerically combined with data from the sandblasted 316L sample as a predictive method. This was done by equating the y intercept of the equation to the emissivity of the sand blasted sample at room temperature, to give emissivity for the interior surfaces of CMF spheres at various angles. The equation used is shown below:

$$y = 1E-11x^6 - 2E-09x^5 + 2E-07x^4 - 1E-05x^3 + 0.0002x^2 - 0.0027x + 0.1697 \quad (1) [9]$$

where y = emissivity of sphere and x = measurement angle

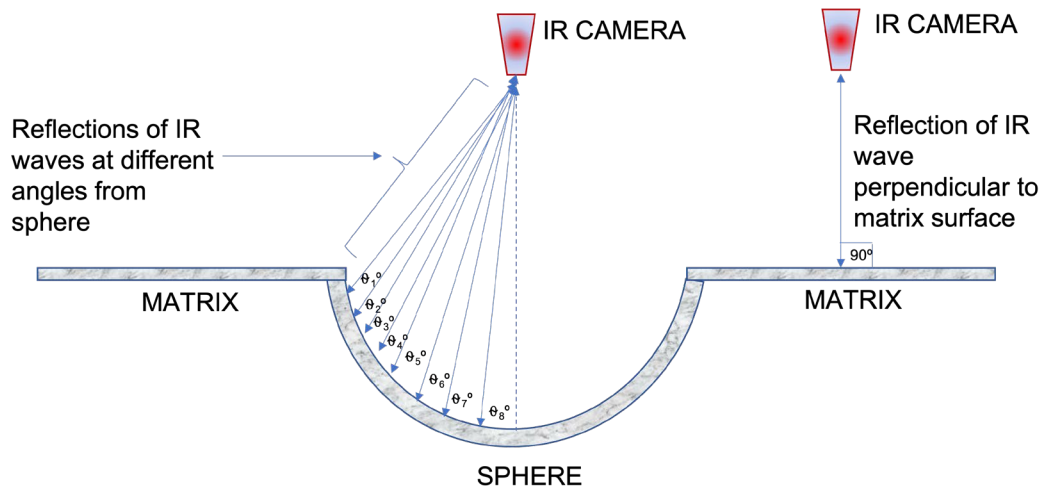


Figure 2. Schematic showing effect of curvature on emissivity data.

4. Results and discussions

4.1 Matrix emissivity

Figure 3 shows measured emissivity of the matrix of the CMF samples at various temperature points and varied surface roughness. It can be observed that the surface emissivity values are decreased with increasing temperature. Also, there is a considerable reduction in the surface

emissivity values as the surface roughness decreases and this is better seen with an increase in temperature. This confirms that the surface roughness directly impacts emissivity.

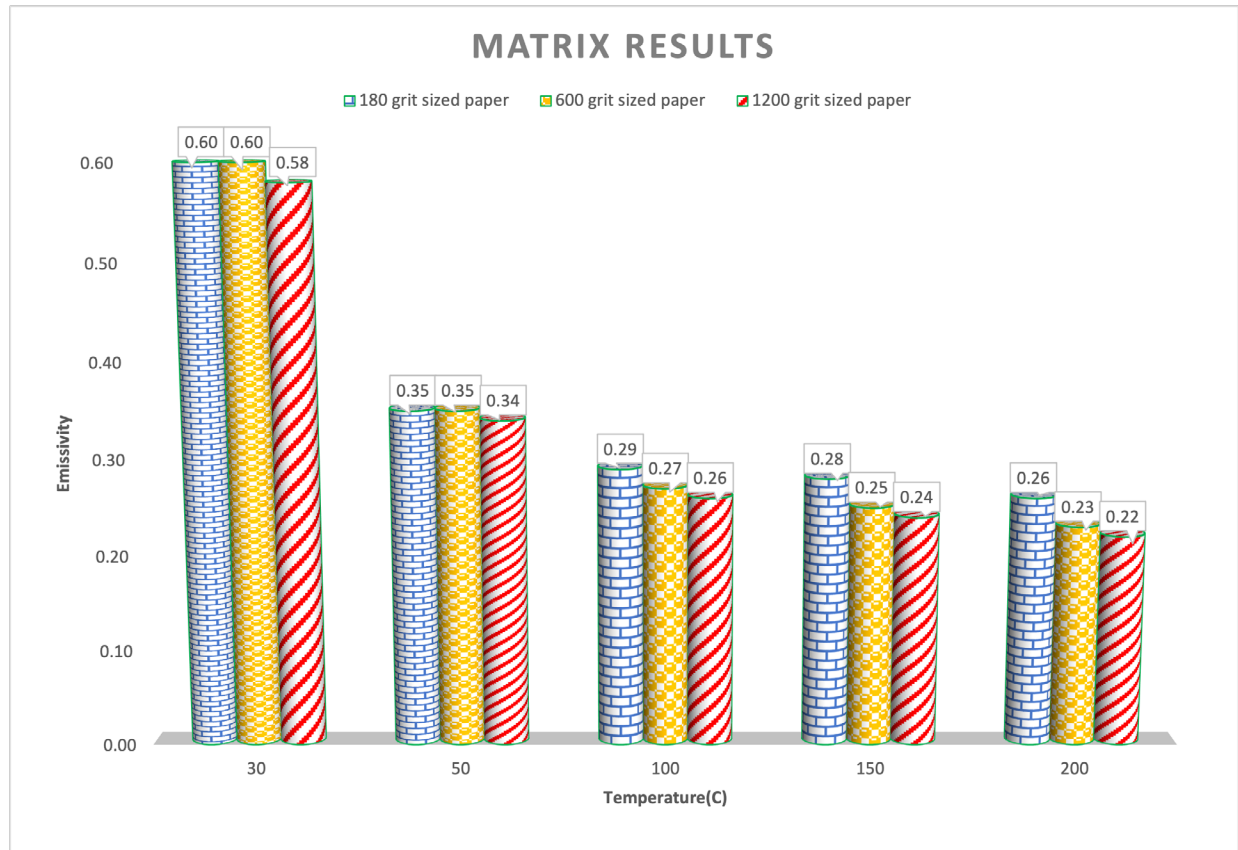


Figure 3. CMF matrix emissivity at various surface roughness and temperatures.

4.2 Sphere emissivity results

Figure 4 shows emissivity results obtained from the sand blasted sample and combined with the effects of spheres angle. It is seen that due to the spheres having a rougher surface profile than that of the matrix, emissivity values obtained here are higher, ranging from 0.5 to 0.99. The angle effects on the sphere emissivity were averaged out and resulting values shown in Table 3. These values become representative of the emissivity of the CMF spheres, which will be applied in the next section for the rule of mixtures.

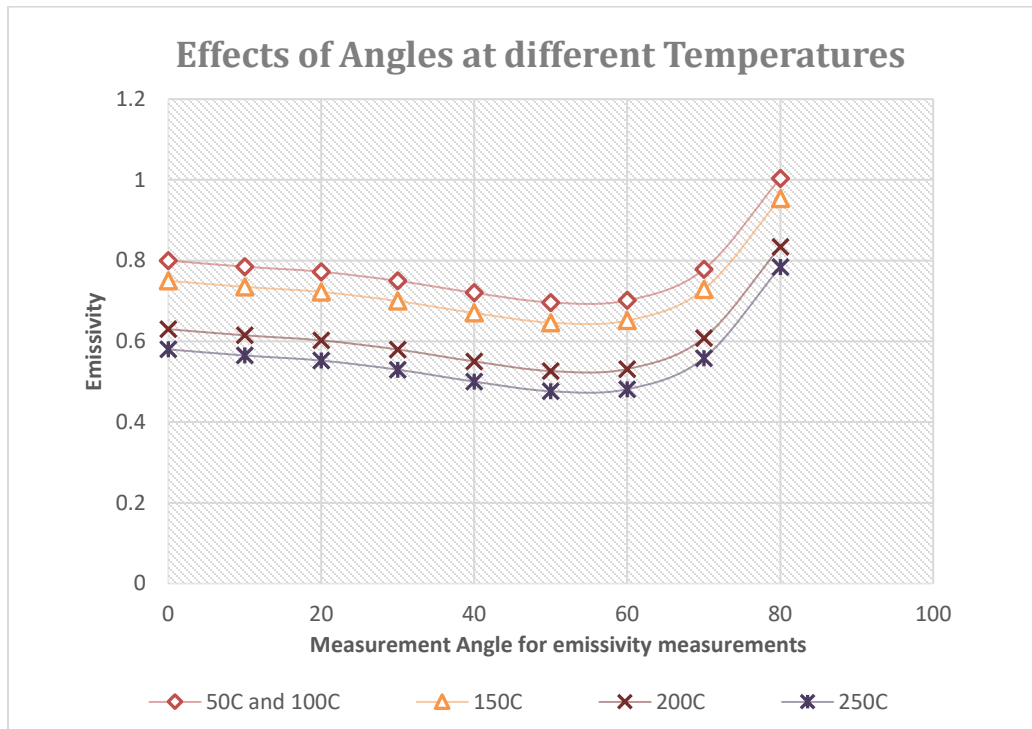


Figure 4. Effects of angle on emissivity of spheres.

Table 3. Averaged emissivity values of CMF spheres.

Average Emissivity of CMF Spheres	
Temperature (°C)	Emissivity
50	0.778
101	0.778
152	0.728
203	0.608
248	0.558

4.3 Rule of mixtures

The lower bound and upper bounds rule of mixtures was applied to the S-S CMF to predict the global surface emissivity of the material based on the emissivity of its components (hollow spheres and the matrix) using the following formula:

$$\text{Upper Bound: } \epsilon_{cmf} = A_{spheres} \cdot \epsilon_{spheres} + A_{matrix} \cdot \epsilon_{matrix} \tag{2}$$

$$\text{Lower Bound: } \epsilon_{cmf} = \frac{1}{\left[\frac{A_{matrix}}{\epsilon_{matrix}} + \frac{A_{sphere}}{\epsilon_{spheres}} \right]} \tag{3}$$

where ϵ = emissivity, A = area.

Using a scanning electron microscope (SEM) image of the CMF sample surface and an image J software the %area of sphere and matrix on a 2 mm sphere CMF sample is estimated (Figure 5(b)).

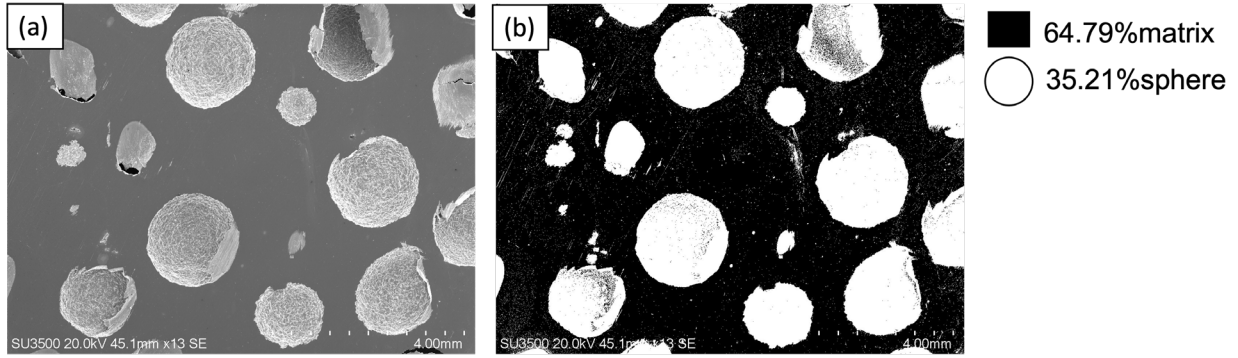


Figure 5. (a) SEM image of CMF sample (b)Image J used to determine %area of spheres and matrix.

After the image J data for area measurements is incorporated into the rule of mixture equations, data was extrapolated to 1200 °C to predict the global surface emissivity of S-S CMF at higher temperatures. Figure 6 shows data obtained. To better understand the graph, “UB” and “LB” represent data for upper-bound and lower-bound emissivity, respectively based on the direct experimental results and shown with scattered graphs. “EXT” represents extrapolated data from 200C to 1200C shown by line graphs. The experimental results were collected from CMF sample surfaces ground at 180, 600 and 1200 grit sizes tested at various temperatures. As can be seen, the emissivity of CMF is directly affected by the roughness of the CMF surface. The smoother the surface is the lower the emissivity value hence data for 1200 grit sized samples show the lowest emissivity values, followed by 600 grit and 180 grit. Emissivity of CMF is also impacted by testing temperature, with higher temperatures showing higher emissivity.

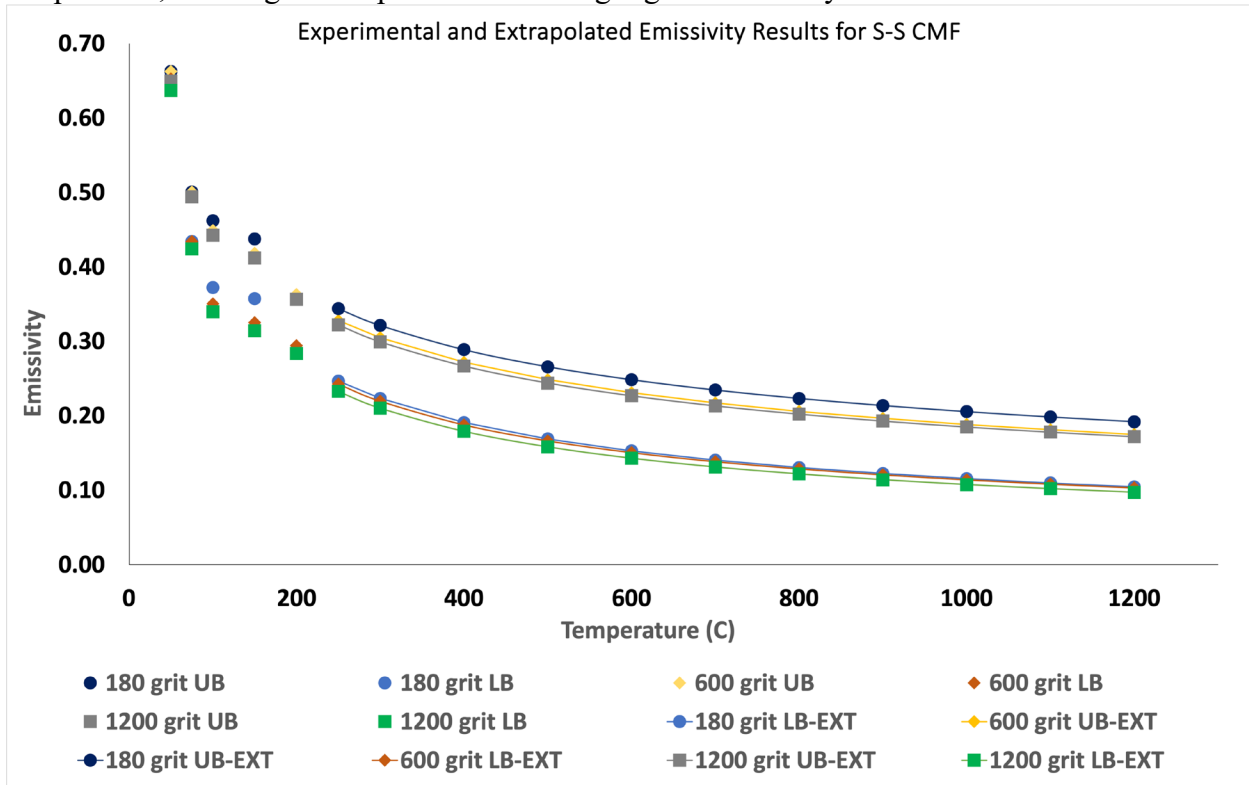


Figure 6. Lower Bound (LB) and Upper Bound(UB) experimental and extrapolated (EXT) surface emissivity values of 2mm sphere S-S CMF for 180, 600 and 1200 grit size at various temperatures.

Conclusion

A systemic approach for the measurement of the surface emissivity of composite materials in general and composite metal foams in particular was successfully developed, and data derived will be applied to a numerical model for a full-scale torch fire test model. Data generated showed that the method developed for finding surface emissivity can predict the surface emissivity of complex composite materials with an easy approach of rule of mixture.

Acknowledgements

This study was supported by the Department of Transportation (DOT) Pipeline and Hazardous Materials Safety Administration (PHMSA) under project number #PH957-20-0075.

References

- [1] United States Department of Transportation, “Tank Car Specifications and Terms,” *Bureau of Transportation Statistics*, Apr. 18, 2018. <https://www.bts.gov/surveys/annual-tank-car-facility-survey/tank-car-specifications-terms>
- [2] Legal Information Institute, Cornell Law School, “49 CFR Part 179- Specifications For Tank Cars.” <https://www.law.cornell.edu/cfr/text/49/part-179>
- [3] A. Rabiei, K. Karimpour, D. Basu, and M. Janssens, “Steel-steel composite metal foam in simulated pool fire testing,” *International Journal of Thermal Sciences*, vol. 153, p. 106336, Jul. 2020. <https://doi.org/10.1016/j.ijthermalsci.2020.106336>
- [4] S. Chen, J. Marx, and A. Rabiei, “Experimental and computational studies on the thermal behavior and fire retardant properties of composite metal foams,” *International Journal of Thermal Sciences*, vol. 106, pp. 70–79, Aug. 2016. <https://doi.org/10.1016/j.ijthermalsci.2016.03.005>
- [5] Nigel Amofo-Yeboah and R. Afsaneh, “Thermal Response of Steel-Steel Composite Metal Foams under Small-Scale Torch-Fire Conditions,” *Advanced Engineering Materials*, May 2023. <https://doi.org/10.1002/adem.202300217>
- [6] B. P. Neville and A. Rabiei, “Composite metal foams processed through powder metallurgy,” *Materials & Design*, vol. 29, no. 2, pp. 388–396, Jan. 2008. <https://doi.org/10.1016/j.matdes.2007.01.026>
- [7] “ASTM E1933-14(2018) Standard Practice for Measuring and Compensating for Emissivity Using Infrared Imaging Radiometers.”
- [8] L. Barker, “Influence of oxidation and emissivity for metallic alloys space debris during their atmospheric entry,” in *7th European Conference on space debris*, Germany, Apr. 2017.
- [9] D. Atasi, “Temperature and angle dependent emissivity and thermal shock resistance off the W/WAIN/WAION/Al₂O₃ based spectrally selective absorber,” *Applied energy materials*, vol. 2, pp. 5557–5567, 2019. <https://doi.org/10.1021/acsaem.9b00743>
- [10] L. Yang and X. Xin-Lin, “Tomography-based analysis of apparent directional spectral emissivity of high porosity nickel foams,” *International Journal of Heat and Mass Transfer*.